(Figure 1).[9] Two Fe(II) atoms are bridged by one monodentate and two bidentate formate ligands. This triply bridged unit represents a new coordination geometry in diiron chemistry, to be contrasted with the known μ-oxo, μ-hydroxo, and μ-phenoxo diiron compounds containing supporting carboxylate bridges.[1,4,5,10] In **1**, a fourth formate ion is coordinated in monodentate fashion to one of the metal centers (Fe1), the octahedral coordination sphere of which is completed by ligation of two imidazoles from a BIPhMe molecule. In contrast, Fe2 is bonded to only five ligands, with a distorted trigonal-bipyramidal geometry.[11] An additional weak interaction occurs with O7 of the monodentate bridging formate [Fe2···O7, 2.74 (1) Å]. The latter is tilted toward Fe2, as reflected by the differing angles Fe1-O1-C3 [133.3 (9)°] and Fe2-O1-C3 [105.4 (7)°]. As expected from the lower coordination number, bonds to Fe2 are shorter than analogous bonds to Fe1 by 0.03-0.07 Å.

The zero-field Mössbauer spectrum of **1** measured at 4.2 K contains a broad, asymmetric doublet that could be nicely fit to a two-site model with δ_1 = 1.26 (3) mm s^{-1}, δ_2 = 1.25 (3) mm s^{-1}, ΔE_{Q1} = 2.56 (3) mm s^{-1}, and ΔE_{Q2} = 3.30 (3) mm s^{-1}. We ascribe the larger quadrupolar splitting to the pentacoordinate iron Fe2, which has the less symmetrical ligand environment. The X-band ESR spectrum at 7 K of a frozen, colorless solution of **1** prepared under N_2 in $CDCl_3$ (5 mM) contains a broad signal at $g \sim 16$ similar to that reported for a phenoxo-bridged diiron(II) complex[4c] and for deoxyHr azide.[2b] In addition, we observe a signal at g = 1.90, the origin of which is under investigation.

Exposure of solutions of **1** in $CHCl_3$ or CH_2Cl_2 to air results in the formation of a green-brown mixture from which green microcrystals of $[Fe_2O(O_2CH)_4(BIPhMe)_2]\cdot H_2O$ (**2**·H_2O) were isolated (~35%).[12] The same material forms upon mixing equimolar quantities of $Fe(O_2CH)_2\cdot 2H_2O$ and BIPhMe in $CHCl_3/CH_3CN$ (1:1) in air. An X-ray crystal structure determination revealed the presence of the now-familiar (μ-oxo)bis(μ-carboxylato)diiron(III) core in **2**, with the terminal metal coordination sites each occupied by two imidazoles from BIPhMe and a monodentate formate ligand cis to the oxo bridge.[13] The geometric parameters from the X-ray structure and the electronic, Mössbauer, IR, and resonance enhanced Raman spectroscopic data for **2** are analogous to those found for oxidized forms of Hr and for other complexes having similar cores.[1,4-6]

The source of the oxo bridge in **2** was determined to be dioxygen, rather than adventitious water, by exposing a solution of **1** in $CHCl_3$ to $^{18}O_2$ and monitoring the symmetric Fe-^{18}O-Fe stretch of the product by resonance enhanced Raman spectroscopy. By comparison to the spectrum of fully ^{18}O labeled **2**, prepared by exchange with $H_2{}^{18}O$, it was evident that ^{18}O incorporation from dioxygen had occurred. Further spectroscopic and mechanistic studies of the reaction of **1** with dioxygen are underway.

In conclusion, with the preparation of **1**, significant progress has been made toward modeling the geometric and spectroscopic properties as well as aspects of the dioxygen reactivity of diiron oxo proteins in their reduced forms. The uniquely bridged diiron(II) compound **1** contains only biomimetic imidazole and carboxylate ligands and a single open coordination site, features of deoxyHr heretofore unknown in synthetic complexes. While reversible dioxygen binding to **1** does not occur in solution at ambient temperature, an oxygen atom is incorporated upon exposure of **1** to air to give **2**. This chemistry is of likely relevance to the formation and/or functional activity of diiron oxo centers in the related proteins ribonucleotide reductase[14] and methane monooxygenase.[15]

Acknowledgment. This work was supported by U.S. Public Health Service Grant GM 32134 from the National Institute of General Medical Sciences. W.B.T. is grateful to the American Cancer Society for a postdoctoral fellowship. A.B. is on sabbatical leave from the Hebrew University of Jerusalem, Israel. We thank Dr. G. C. Papaefthymiou for assistance in obtaining Mössbauer data at the Francis Bitter National Magnet Laboratory, which is supported by the National Science Foundation. We also thank D. P. Bancroft, R. H. Beer, and J. G. Bentsen for assistance.

Supplementary Material Available: Spectroscopic and analytical data for BIPhMe, **1**, and **2**·H_2O, Mössbauer spectrum of **1**, ORTEP diagram and selected bond lengths and angles for **2**·MeOH·H_2O, and tables of atomic positional and thermal parameters for **1**·1.5CH_2Cl_2 and **2**·MeOH·2H_2O (15 pages). Ordering information is given on any current masthead page.

(9) Anal. ($C_{36}H_{40}N_8O_{10}Fe_2$): C, H, N; FTIR (KBr, cm^{-1}) 3122, 2955, 2940, 1609 (s), 1498, 1449, 1358, 1323, 1283, 1071, 988, 897, 762, 725, 702. Crystal data for **1**·1.5CH_2Cl_2 ($C_{37.5}H_{43}N_8O_{10}Cl_3Fe_2$, M_r = 983.86) at 194 K: size ca. 0.2 × 0.2 × 0.1 mm, triclinic, space group $P\bar{1}$ (No. 2), a = 15.47 (1) Å, b = 15.940 (5) Å, c = 10.540 (3) Å, α = 98.72 (2)°, β = 105.38 (5)°, γ = 63.79 (5)°, V = 2246 (4) Å^3, Z = 2, ρ_{calcd} = 1.455 g cm^{-3}. For 3256 unique, observed reflections with $F^2 > 3\sigma(F^2)$ and 455 variable parameters, the current discrepancy indices are R = 0.080 and R_w = 0.100.

(10) Synder, B. S.; Patterson, G. S.; Abrahamson, A. J.; Holm, R. H. *J. Am. Chem. Soc.* **1989**, *111*, 5214 and references therein.

(11) Kepert, D. L. *Inorganic Stereochemistry*; Springer-Verlag: Berlin, 1982, Chapters 4 and 5.

(12) Anal. ($C_{36}H_{42}N_8O_{12}Fe_2$): C, H, N; FTIR (KBr, cm^{-1}) 3424, 3130, 2937, 2832, 1617 (sh), 1590 (s), 1500, 1449, 1356, 1310, 1283, 1070, 988, 900, 762, 725, 704; resonance Raman (λ 406.7 nm, 100 mW, ~0.03 M, $CHCl_3$, cm^{-1}) ν_{sym} (Fe-O-Fe) 518, ν_{sym} (Fe-^{18}O-Fe, by $H_2{}^{18}O$ exchange) 501; UV-vis ($CHCl_3$) [λ_{max}, nm (ϵ_M/Fe cm^{-1} M^{-1})] 329 (3400), 354 (sh, 2900), 448 (370), 478 (sh, 340), 520 (sh), 662 (70); Mössbauer (zero field, 4.2 K, mm s^{-1}) δ 0.54 (3), ΔE_Q 1.81 (3).

(13) Crystal data for **2**·MeOH·2H_2O ($C_{37}H_{48}N_8O_{14}Fe_2$, M_r = 940.53) at 194 K: size 0.20 × 0.15 × 0.15 mm, triclinic, space group $P\bar{1}$ (No. 2), a = 15.215 (6) Å, b = 15.401 (6) Å, c = 10.133 (2) Å, α = 108.70 (3)°, β = 96.41 (2)°, γ = 74.32 (3)°, V = 2165 (3) Å^3, Z = 2, ρ_{calcd} = 1.443 g cm^{-3}, ρ_{measd} = 1.44 (1) g cm^{-3}. For 2629 unique, observed reflections with $F^2 > 3\sigma(F^2)$ and 456 variable parameters, the current discrepancy indices are R = 0.086 and R_w = 0.101. An ORTEP diagram of the complex is presented as supplementary material.

(14) (a) Reichard, P.; Ehrenberg, A. *Science (Washington, D.C.)* **1983**, *221*, 514. (b) Lammers, M.; Follmann, H. *Struct. Bonding* **1983**, *54*, 27.

(15) (a) Woodland, M. P.; Patil, D. S.; Cammack, R.; Dalton, H. *Arch. Biochim. Biophys.* **1986**, *873*, 237. (b) Fox, B. G.; Sererus, K. K.; Münck, E.; Lipscomb, J. D. *J. Biol. Chem.* **1988**, *22*, 10553.

Sequence-Selective Hydrolysis of Duplex DNA by an Oligonucleotide-Directed Nuclease

David R. Corey, Dehua Pei, and Peter G. Schultz*

Department of Chemistry
University of California, Berkeley
Berkeley, California 94720

Received May 23, 1989

The design of molecules capable of the efficient sequence-specific cleavage of large double-stranded DNAs would greatly facilitate the manipulation and mapping of genomic DNA. Current strategies for the selective cleavage of large duplex DNAs include the use of triple-helix formation[1] and DNA-binding proteins[2] to deliver oxidative cleaving agents to the sequence of interest. We report here the sequence-specific hydrolysis of supercoiled double-stranded DNA by a hybrid nuclease consisting of a short oligonucleotide selectively fused to staphylococcal nuclease.[3] Plasmid pUC19[4] was partially denatured in order to facilitate hybridization of the oligonucleotide-enzyme adduct[5] to DNA via D-loop formation[6] (Figure 1a). Both strands of the substrate were then efficiently hydrolyzed by the bound hybrid

* Author to whom correspondence should be addressed.

(1) (a) Stroebel, S. A.; Moser, H. E.; Dervan, P. B. *J. Am. Chem. Soc.* **1988**, *110*, 7927. (b) Francois, J.; Saison-Behmoaras, T.; Chassignol, M.; Thuong, N. T.; Helene, C. *J. Biol. Chem.* **1989**, *264*, 5891.

(2) (a) Mack, D. P.; Iverson, B. L.; Dervan, P. B. *J. Am. Chem. Soc.* **1988**, *110*, 7572. (b) Chen, B. C.; Sigman, D. S. *Science* **1987**, *237*, 1197.

(3) Tucker, P.; Cotton, F.; Hazen, E. *Mol. Cell. Biochem.* **1979**, *23*, 67.

(4) Yanisch-Perron, C.; Viera, J.; Messing, J. *Gene* **1985**, *33*, 103.

(5) Landgren, U.; Kaiser, R.; Sanders, J.; Hood, L. *Science* **1988**, *241*, 1077. (b) Wang, Y. *Biotechniques* **1988**, *6*, 843.

(6) Wiegand, R. C.; Beattie, K. L.; Holloman, W. K.; Radding, C. M. *J. Mol. Biol.* **1977**, *116*, 805.

0002-7863/89/1511-8523$01.50/0

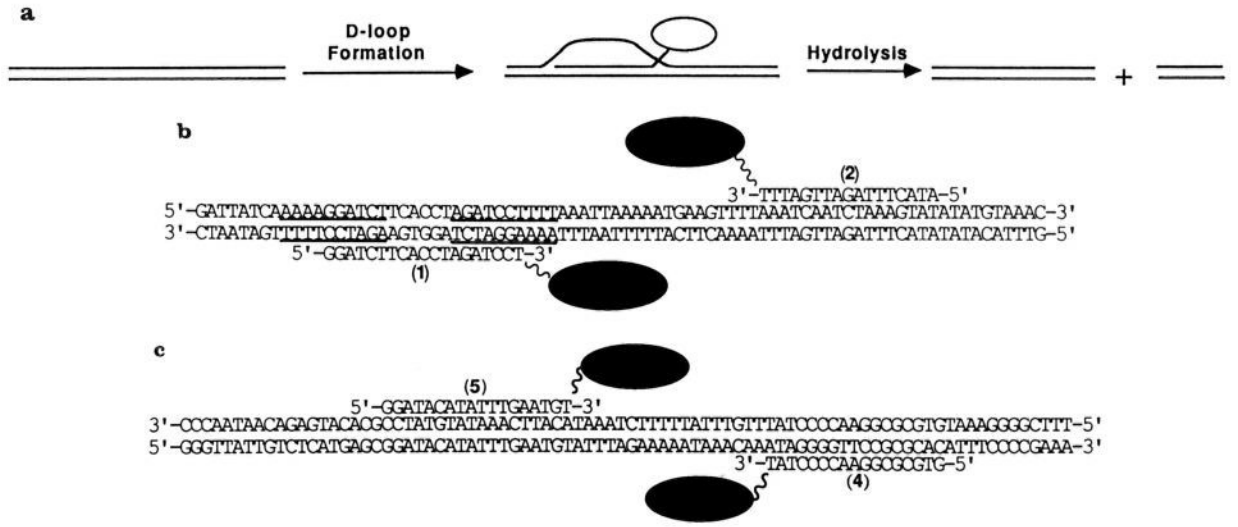

Figure 1. (a) Scheme showing D-loop formation and subsequent hydrolysis. (b) Scheme showing the alignment of hybrid nucleases **1** and **2** with pUC19 (bases 1532–1613). The underlined bases form a 10-base hairpin stem structure. (c) Scheme showing the alignment of **4** and **5** with pUC19 (bases 2523–2658).

nuclease. This represents *a significant new strategy* for the delivery of chemically reactive probes to defined sequences within supercoiled DNA.

Hybrid nucleases were constructed via a disulfide exchange reaction between a cysteine-containing mutant of staphylococcal nuclease (K84C)[7] and either a 19-nucleotide (**1**) or 17-nucleotide (**2**) oligomer containing a 3′-*S*-pyridylthiodisulfide.[8-10] The K84C nuclease was linked directly to the 3′-thiol group of the terminal thymidine.[9,10]

The ability of the hybrid nucleases to sequence-specifically hydrolyze supercoiled DNA was assayed with pUC19, a 2686-base-pair plasmid.[4] The sequences of the oligonucleotide binding domains for the two hybrid nucleases were chosen so that they would deliver the attached nuclease to either side of a thymidine-rich site within the plasmid (Figure 1b) (the cleavage preference of staphylococcal nuclease is T ≫ A > C, G[9]). Plasmid pUC19 (1 μg, 0.031 μM, 82 μM in base pairs) was partially denatured by incubation with 3.5 mM NaOH.[11] After neutralization, the hybrid nuclease was added to allow hybridization with substrate. The nuclease was then activated by the addition of Ca^{2+} (the enzyme is completely dependent on Ca^{2+} for activity). Cleavage was terminated after 5 s by the addition of ethylene glycol bis(1-aminoethyl ether)-*N*,*N*,*N*′,*N*′-tetraacetic acid (EGTA).

In order to elucidate the extent and location of specific cleavage, the reaction products were treated with the restriction enzyme *Hin*d III in order to generate discrete fragments whose sizes could be compared to known standards (the hybridization conditions do not impair the ability of duplex DNA to be cleaved by a restriction enzyme). Inspection of an ethidium bromide stained agarose gel reveals that both the 17 nt and 19 nt hybrid nucleases cleave substrate at the predicted target site (Figure 2).[13] Hydrolysis by the hybrid nucleases and *Hin*d III produces two fragments (predicted fragment sizes ~1123 and ~1563 base pairs), which can be compared to those from a *Bgl* I digest (1118 and 1568 base pairs). The 19-nt hybrid nuclease hydrolyzed DNA more efficiently than the 17-nt nuclease, possibly due to the presence of a 10-nt hairpin stem structure at the 19-nt binding site which may encourage hybridization (Figure 1b). Control experiments showed that neither free enzyme alone nor free enzyme in combination with free 19-nt oligonucleotide produced specific cleavage. Likewise, hybrid nuclease **3**,[14] which was

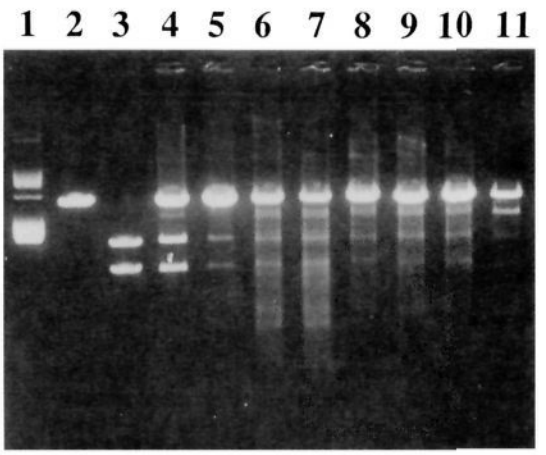

Figure 2. A 1% ethidium bromide stained agarose gel. Lanes 2 and 4–11 were treated with *Hin*d III: lane 1, pUC19; lane 2, pUC19 linearized with *Hin*d III; lane 3, pUC19 digested with *Bgl* I; lane 4, pUC19 digested with **1** (0.06 μM); lane 5, pUC19 digested with **2** (0.06 μM); lane 6, pUC19 digested by free K84C staphylococcal nuclease (0.2 μM); lane 7, pUC19 digested by K84C staphylococcal nuclease (0.2 μM) in the presence of free 19-nt oligonucleotide (0.3 μM); lane 8, pUC19 digested with **3** (0.2 μM); lane 9, pUC19 digested with **4** (0.2 μM); lane 10, pUC19 digested with **5** (0.2 μM); lane 11, pUC19 digested by **4** (0.1 μM) and **5** (0.1 μM) in tandem. Denaturation, annealing, and cleavage conditions: to 12 μL of a 3.5 mM solution of aqueous sodium hydroxide was added 1 μg of pUC19. After incubation for 10 min at 37 °C, 50 mM HCl was added to neutralize the solution, followed by addition of nuclease. Hybrid nuclease and pUC19 (0.031 μM) were annealed for 10 min at 37 °C, in a total volume of 20 μL. The mixture was then cooled to 20 °C, and buffer was added to make the solution 35 mM in NaCl and 25 mM in Bis-Tris, pH 6.5. Cleavage was initiated by the addition of $CaCl_2$ to a final concentration of 2 mM and was terminated after 5 s by the addition of EGTA to a final concentration of 5 mM. The reaction products were precipitated with ethanol and then treated with 5 units of *Hin*d III prior to analysis by agarose gel electrophoresis.

(7) V_{max} for the K84C nuclease was 0.15 Δabs_{260} min^{-1} (μg nuclease)$^{-1}$, K_m was 18.6 μg of DNA/mL. Determined by the method of Serpersu et al.: Serpersu, E. H.; Shortle, D.; Mildvan, A. S. *Biochemistry* **1987**, *26*, 1289.

(8) (a) Zuckermann, R.; Corey, D.; Schultz, P. *Nucleic Acids Res.* **1987**, *15*, 5305. (b) Corey, D. R.; Schultz, P. G. *Science* **1987**, *238*, 1401.

(9) Corey, D. R.; Pei, D.; Schultz, P. G. *Biochemistry*, in press.

(10) The controlled pore glass used for oligonucleotide synthesis was derivatized with 3′-mercapto-5′-*O*-(4,4′-dimethoxytrityl)thymidine.[9]

(11) Treatment of *Saccharomyces cerevisiae* chromosomal DNA with <20 mM NaOH does not effect DNA mobility during pulsed-field gel electrophoresis.

(12) Hybrid nuclease synthesized with oligonucleotide **1** selectively cleaved DNA without prior denaturation with base, indicating that either secondary structure at the site or some other factor allows exceptionally facile hybridization and cleavage; see: Dingall, C.; Lomonossoff, G. P.; Laskey, R. A. *Nucleic Acids Res.* **1981**, *12*, 2659.

(13) Hybrid nucleases that contained the K116C mutation functioned similarly.

synthesized with an oligonucleotide that was not complementary to any site in pUC 19, failed to hydrolyze DNA selectively. Neither a 17-nt (**4**) nor an 18-nt (**5**) hybrid nuclease designed to deliver the nuclease to a second site within pUC 19 (Figure 2c) was able to selectively hydrolyze that site. Lack of cleavage may be due to unfavorable secondary structure that prevents hybridization, or to inefficient cleavage of both strands by the bound hybrid nuclease. Simultaneous addition of **4** and **5** to the reaction mixture afforded selective cleavage (fragment sizes ~2120 and ~566 base pairs), possibly because each nuclease was required to hydrolyze only one strand of the duplex. The introduction of additional supercoiling into pUC19 with topoisomerase I and ethidium bromide[15] substantially enhances selective cleavage by hybrid nucleases **2**, **4**, and **5**.

This work illustrates that supercoiled DNA can be sequence-specifically hydrolyzed with a hybrid nuclease delivered via D-loop formation. The hydrolysis is relatively efficient and can be carried out on a preparative scale. The generality of this approach with respect to DNA sequence and structure remains to be determined. Nevertheless, this is an important step toward the development of strategies for cleaving large linear duplex DNAs.

Acknowledgment. Support for this work was provided by the National Institutes of Health (1R01GM41679-01). We also thank the referees for their helpful comments.

(14) Binding domain oligonucleotide: 5'-CTTATTTGGATTGGGAT-3'.
(15) Franklin, P. B.; Schutte, B. C.; Cox, M. M. *J. Mol. Biol.* **1989**, *205*, 487.

Observation of Spin Diffusion in Biomolecules by Three-Dimensional NOE-NOE Spectroscopy

R. Boelens,* G. W. Vuister, T. M. G. Koning, and R. Kaptein

Department of Chemistry, University of Utrecht Padualaan 8, 3584 CH Utrecht, The Netherlands

Received June 12, 1989

The nuclear Overhauser effect (NOE) between two protons is one of the most useful NMR parameters for structural studies of biomolecules in solution.[1] It forms the basis for the methods of sequential resonance assignment in ^{1}H NMR spectra of biomolecules, and it is the source of distance constraints necessary in the structure determination.

For small rigid molecules, the NOE, which is due to dipolar cross-relaxation between the protons,[2] is simply related to the inverse 6th power of the proton-proton distance. Thus measurements of NOE intensities lead in a direct way to relative distances, which can be calibrated by using known distances.[3] However, for large molecules the cross-relaxation pathways via other protons contribute to the NOE between two protons as well.[4] In analogy with similar effects in solid-state NMR, this indirect magnetization transfer is often called spin diffusion.[4,5] Because of the uncertainties due to spin diffusion and the motional behavior of the biomolecule, the NOE is often used to derive just approximate distances.

In the past, several methods have been developed to obtain more accurate distances from NOE data. Instead of recording steady-state NOEs, it was proposed to measure NOE buildup rates after short irradiation times or by transient techniques.[6,7] In the case of biomolecules, the NOE is nowadays generally measured by two-dimensional (2D) NOE spectroscopy,[1,8,9] a method related to the 1D transient technique. Furthermore, for these 2D methods it was preferred to use short mixing times or to use a series of mixing times to extract the initial buildup rate.[10,11] Recently, Olejniczak et al.[12] proposed to irradiate the intermediate spin in the mixing time of a 2D NOE experiment and to estimate in that way the contribution of the indirect magnetization transfer to the NOE. Other approaches used to reduce the effects of spin diffusion are based on the back transformation of the complete NOE matrix, to obtain the relaxation matrix directly.[12,13] For biomolecules, where it is difficult to assign the complete NOE matrix, this procedure can be combined with restrained molecular dynamics to reduce iteratively the effects of spin diffusion.[14]

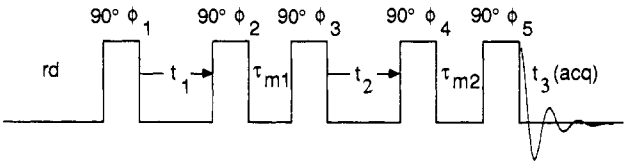

Figure 1. Pulse scheme of the 3D NOE-NOE experiment. Saturation of the HOD line was achieved by low-power irradiation during the relaxation delay, RD, and the two mixing times, τ_{m1} and τ_{m2}. The frequency for the rf pulses and the decoupling was derived from one synthesizer. The phase cycling used is as follows: $\phi_1 = x, -x, y, -y$; $\phi_2 = 2(-x), 2(-y)$; $\phi_3 = 2(-x), 2(-y), 2(x), 2(y)$; $\phi_4 = 2(x), 2(y)$; $\phi_5 = 2(x), 2(-y)$; acq = $x, -x, -y, y, -x, x, y, -y$. TPPI was applied independently for the t_1 and t_2 domains on ϕ_1 and ϕ_3.

Recently, a number of 3D NMR experiments have been reported, such as the homonuclear 3D *J*-resolved experiment,[15] 3D soft COSY-COSY,[16] soft NOESY-COSY,[17] soft NOESY-HOHAHA,[18] nonselective 3D NOE-HOHAHA,[19] HMQC-COSY,[20] and HMQC-NOESY.[20-22] Most of these experiments were motivated by the resulting reduction of overlap on adding a third frequency domain to the 2D NMR spectrum. In addition, as pointed out by Griesinger et al.,[16] the 3D cross-peaks in a COSY-COSY experiment can reveal unambiguously two-step *J* connectivities. Similarly, in the present communication we want to stress the observation of such second-order magnetization transfer for the NOE by the 3D NOE-NOE experiment.

The pulse scheme of the 3D NOE-NOE experiment (Figure 1) reveals two mixing periods separating two evolution periods and a detection period. In each mixing time, the magnetization

(1) Wüthrich, K. *NMR of proteins and nucleic acids*; John Wiley and Sons: New York, 1986.
(2) Solomon, I. *Phys. Rev.* **1955**, *99*, 559-565.
(3) Noggle, J. H.; Schirmer, R. E. *The nuclear Overhauser effect. Chemical applications*; Academic Press: New York, 1971.
(4) Kalk, A.; Berendsen, H. J. C. *J. Magn. Reson.* **1976**, *24*, 343-366.
(5) Abragam, A. *The Principles of Nuclear Magnetism*; Clarendon Press: Oxford, 1961; pp 136-144.
(6) Wagner, G.; Wüthrich, K. *J. Magn. Reson.* **1979**, *33*, 675-680.
(7) Dobson, C. M.; Olejniczak, E. T.; Poulsen, F. M.; Ratcliffe, R. G. *J. Magn. Reson.* **1982**, *48*, 97-110.
(8) Jeener, J.; Meier, B. H.; Bachmann, P.; Ernst, R. R. *J. Chem. Phys.* **1979**, *71*, 4546-4553.
(9) Ernst, R. R.; Bodenhausen, G.; Wokaun, A. *Principles of Magnetic Resonance in One and Two Dimensions*; Clarendon Press: Oxford, 1987.
(10) Kumar, A.; Wagner, G.; Ernst, R. R.; Wüthrich, K. *J. Am. Chem. Soc.* **1981**, *103*, 3654-3658.
(11) Scheek, R. M.; Boelens, R.; Russo, N.; Kaptein, R. *Biochemistry* **1984**, *23*, 1371-1376.
(12) Olejniczak, E. T.; Gampe, R. T., Jr.; Fesik, S. W. *J. Magn. Reson.* **1986**, *67*, 28-41.
(13) Fesik, S. W.; O'Donnell, T. J.; Gampe, R. T., Jr.; Olejniczak, E. T. *J. Am. Chem. Soc.* **1986**, *108*, 3165-3170.
(14) Boelens, R.; Koning, T. M. G.; van der Marel, S. A.; van Boom, J. H.; Kaptein, R. *J. Magn. Reson.* **1989**, *82*, 290-308.
(15) Vuister, G. W.; Boelens, R. *J. Magn. Reson.* **1987**, *73*, 328-333.
(16) Griesinger, C.; Sørensen, O. W.; Ernst, R. R. *J. Magn. Reson.* **1987**, *73*, 574-579.
(17) Griesinger, C.; Sørensen, O. W.; Ernst, R. R. *J. Am. Chem. Soc.* **1987**, *109*, 7227-7228.
(18) Oschkinat, H.; Griesinger, C.; Kraulis, P. J.; Sørensen, O. W.; Ernst, R. R.; Gronenborn, A.; Clore, G. M. *Nature* **1988**, *332*, 374-376.
(19) Vuister, G. W.; Boelens, R.; Kaptein, R. *J. Magn. Reson.* **1988**, *80*, 176-185.
(20) Fesik, S. W.; Zuiderweg, E. R. P. *J. Magn. Reson.* **1988**, *78*, 588-593.
(21) Marion, D.; Kay, L. E.; Sparks, S. W.; Torchia, D. A.; Bax, A. *J. Am. Chem. Soc.* **1989**, *111*, 1515-1517.
(22) Zuiderweg, E. R. P.; Fesik, S. W. *Biochemistry* **1989**, *28*, 2387-2391.

0002-7863/89/1511-8525$01.50/0